AD-A159 470 IDENTIFICATION AND VERIFICATION OF FREQUENCY-DOMAIN MODELS FOR XV-15 TILT (U) NATIONAL AERONAUTICS AND SPACE ADMINISTRATION MOFFETT FIELD C

1/1

UNCLASSIFIED M B TISCHLER ET AL AUG 84 NASA-A-9851 F/G 1/3 NL

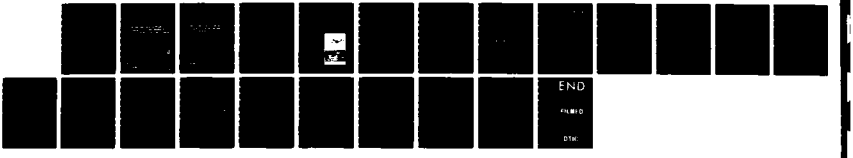

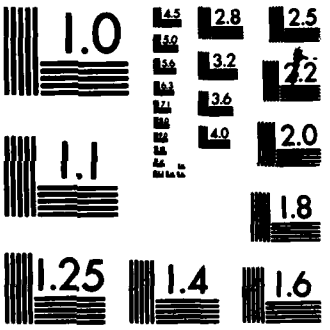

MICROCOPY RESOLUTION TEST CHART
NATIONAL BUREAU OF STANDARDS-1963-A

NASA Technical Memorandum 86009

TM-84-A-6

Identification and Verification of Frequency-Domain Models for XV-15 Tilt-Rotor Aircraft Dynamics

Mark B. Tischler, Joseph G.M. Leung
and Daniel C. Dugan

August 1984

NASA
National Aeronautics and Space Administration

United States Army Aviation Systems Command

NASA Technical Memorandum 86009 TM-84-A-6

Identification and Verification of Frequency-Domain Models for XV-15 Tilt-Rotor Aircraft Dynamics

Mark B. Tischler, Aeromechanics Laboratory, U. S. Army Research & Technology Laboratory, AVSCOM, Moffett Field, California
Joseph G. M. Leung,
Daniel C. Dugan, Ames Research Center, Moffett Field, California

National Aeronautics and Space Administration
Ames Research Center
Moffett Field, California 94035

United States Army Aviation Systems Command
St. Louis, Missouri 63120

IDENTIFICATION AND VERIFICATION OF FREQUENCY-DOMAIN MODELS FOR XV-15 TILT-ROTOR AIRCRAFT DYNAMICS

Mark B. Tischler
Aeromechanics Laboratory, U.S. Army Research and Technology Laboratories (AVSCOM)
Ames Research Center, Moffett Field, California 94035 U.S.A.

Joseph G. M. Leung and Daniel C. Dugan
NASA Ames Research Center, Moffett Field, California 94035 U.S.A.

Abstract

Frequency-domain methods are used to extract the *open-loop* dynamics of the XV-15 tilt-rotor aircraft from flight test data for the cruise condition (V = 170 knots). The frequency responses are numerically fitted with transfer-function forms to identify equivalent modal characteristics. The associated handling quality parameters meet or exceed Level II, Category A, requirements for fixed-wing military aircraft. Step response matching is used to verify the time-domain fidelity of the transfer-function models for the cruise and hover flight conditions. The transient responses of the model and aircraft are in close agreement in all cases, except for the normal acceleration response to elevator deflection in cruise. This discrepancy is probably due to the unmodeled rotor rpm dynamics. The utility of the frequency-domain approach for dynamics identification and analysis is clearly demonstrated.

1. Introduction

The identification of XV-15 tilt-rotor dynamics (Fig. 1) from flight test data is an extensive ongoing effort to support the development of the next generation of tilt rotors—the joint services V/STOL aircraft (JVX). The key concerns of the effort are the documentation of open-loop XV-15 dynamics, and the validation of generic tilt-rotor models (Refs. [1] and [2]). A frequency domain-based identification approach was developed and successfully applied for the hover flight condition (Ref. [3]). Transfer function models describing the open-loop response characteristics of the XV-15 aircraft were extracted and compared with the simulation characteristics. Reference [3] presents a detailed description of the frequency-domain methodology and the results for the hover flight condition.

As in all identification research, a key concern of this effort is the fidelity of the extracted models for input forms other than those used in the identification process. The flight testing technique of Ref. [3] uses a pilot-generated swept sine wave input to excite the vehicle dynamics. This yields an excellent identification of frequency responses and transfer functions for sinusoidal-like inputs. Such information is useful for frequency domain-based handling quality specifications such as the Mil Handbook for military aircraft (Ref. [4]). However, for time-domain specifications such as Mil-H-8501 (Ref. [5]) and Mil-F-83300 (Ref. [6]), criteria are largely based on responses to step inputs, so extracted models must accurately reflect these characteristics as well.

Figure 1. The XV-15 Tilt-Rotor Aircraft. (a) Cruise configuration. (b) Hover configuration.

This paper reviews the frequency-domain based methodology and discusses the identification of transfer function models for the cruise flight condition (170 knots). This is a good limiting case for comparison with the previous hover results (Ref. [3]). Time-domain matching is presented to verify the step response characteristics of the extracted models for the hover and cruise flight conditions. These results show the utility of relatively simple transfer function models for handling qualities and control system applications.

2. Review of Identification Methodology

This section reviews the frequency-domain identification and time-domain verification techniques. The details of the identification approach are extensively discussed in Ref. [3] and are only outlined in this paper.

Frequency-domain identification is based on the spectral analysis of input and output time histories using Fast Fourier Transform techniques. This analysis produces describing functions which are (complex-valued) linear descriptions of the input-to-output processes. The identification results are presented in Bode plot format: magnitude and phase versus frequency. System bandwidth and effective time delay, important metrics in current handling qualities specifications, can be read directly from these plots. Tabulated frequency response results are fitted with analytical transfer function forms to extract modal characteristics for handling qualities specifications given in terms of lower order (equivalent) system models. Also, the transfer-function models can be driven with step inputs to extract familiar time domain metrics such as rise time, overshoot, and settling time.

The swept sine wave (frequency-sweep) input is a good excitation for the frequency-domain identification approach. This excitation results in bounded and reasonable excursions of the aircraft, suitably exciting the important rigid body modes over the entire frequency range of interest (0.2-6.0 rad/sec). The input is generated by the pilot in one axis at a time, with minimal regulation of the remaining axes. Starting from a trim condition, the pilot first executes two 20 sec period inputs to ensure good low-frequency identification. Then the frequency of the inputs is slowly increased up to a maximum of about 6 rad/sec, yielding a total run length of about 90 sec. Repeat runs are executed to allow concatenation of the 90 sec records in the analysis; this technique minimizes the effects of random noise.

When the bare airframe characteristics of the vehicle are highly unstable, as in the XV-15 in hover, execution of a 90 sec frequency sweep on the open-loop vehicle is clearly not practical. Subject to some important qualifications, the bare airframe transfer functions can be extracted from the closed-loop flight data. Referring to Fig. 2, identification of the open-loop transfer function (q/δ_e) requires the measurement of the output (q) and surface deflection (δ_e) signals. This total surface deflection is made up of components from the pilot (δ_{LON}) and the stability and control augmentation system (SCAS) feedback (δ_{f_e}). A key requirement is that the total surface deflection must contain a significant component from the pilot which is uncorrelated with the output. The use of the "programmed" swept sine wave input avoids the otherwise troublesome result of identifying the inverse feedback transfer function ($-1/G_{F_q}$) from passive tracking tasks.

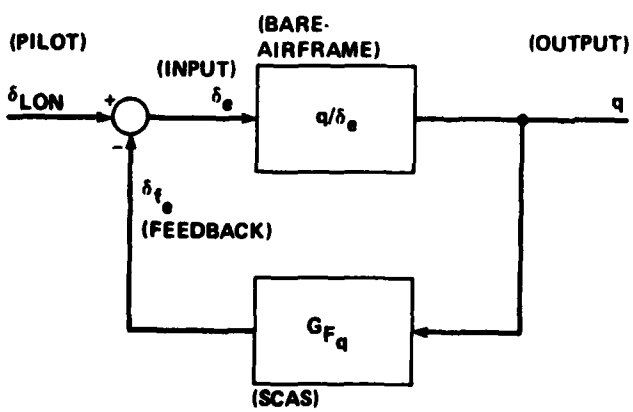

Figure 2. Single degree-of-freedom pitch response model.

When the vehicle dynamics are highly coupled, multiple control deflections will occur in all degrees of freedom. If the surface deflections are *not fully correlated* with each other, the desired single-input transfer function can be isolated using the multi-input multi-output methodology described in Ref. [3]. This restriction was satisfied for the hover flight condition since the cross-control inputs supplied by the pilot were largely uncorrelated with the primary frequency sweep inputs. Therefore, it was possible to isolate the yaw response to ailerons—an important source of coupling for the hover flight condition.

For the cruise flight condition, open-loop longitudinal transfer functions were also identified from the closed-loop tests since the elevator inputs supplied by the pilot were uncorrelated with the outputs and the other surface deflections. In the lateral axis, the large degree of inherent closed-loop stability allowed the pilot to execute frequency sweeps of the aileron without applying rudder corrections. However, the stability augmentation system supplies

rudder inputs which are highly correlated to the aileron inputs and roll rate outputs. Therefore, extraction of the single-input, single-output open-loop transfer functions from closed-loop flight data was not possible for this flight condition; the lateral-directional tests were repeated with the SCAS disengaged. When the bare airframe dynamics are too highly coupled or unstable to make this practical, the open-loop dynamics can usually be extracted from the closed-loop test data, as was successfully accomplished for the XV-15 in hover (Ref. [3]).

Once the flight data have been digitized and preprocessed, the input, output, and cross spectra ($G_{xx}(f)$, $G_{yy}(f)$, and $G_{xy}(f)$, respectively) are calculated using modern Chirp z-transform methods (Ref. [3]). Specific transfer functions $G(f)$ are obtained from the ratio of the appropriate cross and input auto spectra:

$$G(f) = \frac{G_{xy}(f)}{G_{xx}(f)} \tag{1}$$

and are presented in Bode format. The coherence function (γ^2_{xy}) defined as:

$$\gamma^2_{xy} = \frac{|G_{xy}|^2}{|G_{xx}||G_{yy}|} \tag{2}$$

is a good indication of the input-to-output linearity. This frequency-dependent parameter may be interpreted as that fraction of the output spectrum which can be accounted for by linear relation with the input spectrum. When the process under investigation is perfectly linear and the spectral estimates are noise free, the coherence function will be unity for all frequencies in the excited input spectrum range. A value of the coherence function less than unity will result from nonlinearities in the system, input/output noise, or cross-coupled control inputs. The magnitude and phase responses are then fitted with analytical transfer function models to obtain closed form descriptions of the input-to-output processes. In order to obtain a unique fit of the frequency responses, certain physical restraints on commonality of the transfer function denominator factors are imposed.

Current military handling quality specifications (Ref. [4]) limit the allowable mismatch between the transfer function fits and the frequency response data. However, even small decibel deviations in the frequency-domain can produce surprisingly large discrepancies in time-domain correlations. Time-domain verification first requires converting the transfer functions to canonical form:

$$\left.\begin{aligned} \dot{\underline{x}}(t) &= F\underline{x}(t) + G\underline{u}(t) \\ \underline{y}(t) &= C\underline{x}(t) \end{aligned}\right\} \tag{3}$$

where

$$F = \begin{bmatrix} 0 & 1 & 0 & \cdots & 0 \\ 0 & 0 & 1 & \cdots & 0 \\ \vdots & & & & \\ -a_0 & -a_1 & -a_2 & & -a_{n-1} \end{bmatrix} \qquad G = \begin{bmatrix} 0 \\ 0 \\ \vdots \\ 1 \end{bmatrix}$$

$$C = \begin{bmatrix} b_0 & b_1 & \cdots & b_m & 0 & \cdots & 0 \end{bmatrix}$$

and $a_0, a_1, \ldots, a_{n-1}$ are the denominator (ascending) coefficients and $b_0, b_1, \ldots, b_m$ are the numerator (ascending) coefficients of the transfer function model being evaluated.

This model is driven with step-input data from the flight tapes, and the resulting responses are then compared to the aircraft data for time-domain fidelity. This approach allows the verification of transfer functions associated with the *stable* degrees of freedom, since spurious model inputs (due to inexact initial condition matching and turbulence regulation) do not cause a divergence of the transients with time. However, for the *unstable* degrees of freedom, these spurious inputs cause a rapid divergence of the flight and model responses. For such cases, conclusive quantitative statements on the step response fidelity of the transfer function models cannot be made, even though the qualitative form of the response is correct and small differences in the predicted level of instability are probably not important.

3. Dynamics Identification for the Cruise Flight Condition

In this section, the characteristics for the cruise flight condition are considered: V = 170 knots (indicated), nacelle incidence = 0°, altitude = 8000 ft. The longitudinal and lateral flight dynamics are fully decoupled in this condition. The primary longitudinal bare-airframe transfer functions of interest are pitch rate and normal acceleration responses to elevator deflection, q/δ_e and a_z/δ_e, respectively. The important lateral-directional transfer functions are roll rate response to aileron, p/δ_a, and sideslip (at the c.g.) response to rudder, β_{cg}/δ_r.

The following discussion of longitudinal dynamics identification and analysis is presented in detail to illustrate the frequency-domain methodology and to compare the longitudinal results for the hover flight condition presented in Ref. [3].

Longitudinal Dynamics

Since the longitudinal and lateral dynamics are fully decoupled and elevator surface deflections are measured directly, the flight testing for the longitudinal axis was conducted with the SCAS engaged. This was not considered essential, however, since the dynamics for this flight condition are very stable.

The longitudinal stick displacements for two concatenated frequency sweeps are shown in Fig. 3. As previously discussed, each run lasts roughly 90 sec and is initiated with two 20-sec cycles to ensure good low-frequency identification. The sinusoidal stick deflection is very regular with a nearly constant amplitude of roughly ±5%. The elevator signal is also very regular with a nearly constant amplitude of 2 deg. These data are very typical of the transition-flight and forward-flight condition results. The relative stability of the longitudinal and lateral axes made execution of the frequency sweeps a very rapid and acceptable flight-test procedure. The input autospectrum for the concatenated elevator time histories is shown in Fig. 4. This spectrum is fairly flat at low frequencies, dropping off slightly for the higher frequency inputs. For frequencies outside the plotted range, the magnitude drop-off is much more pronounced.

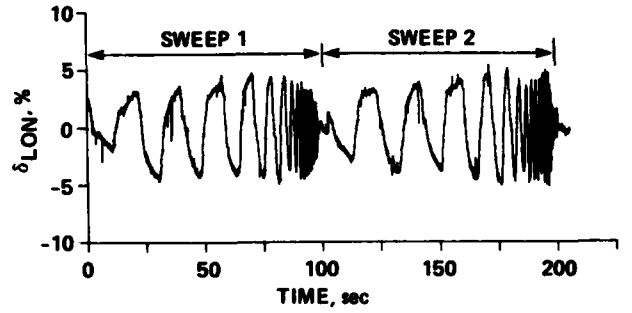

Figure 3. Two longitudinal stick frequency sweeps (δ_{LON}) in cruise.

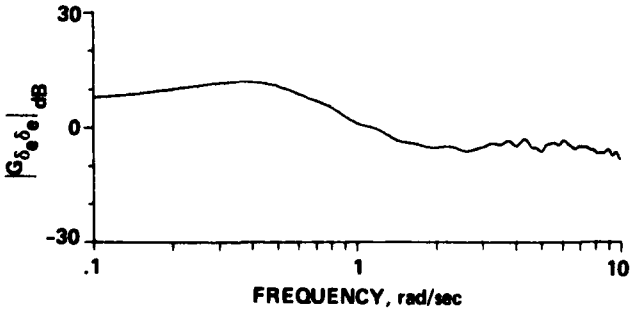

Figure 4. Elevator surface input autospectrum ($G_{\delta_e\delta_e}$).

The pitch-rate signal (conditioned with a 2.5 Hz low-pass filter for output presentation only) is shown in Fig. 5. The pitch-rate excursions are very regular with a roughly constant peak-to-peak amplitude of 5 deg/sec. These oscillations are considered very acceptable to the research pilots, and are comparable with those encountered during the hover flight test. The associated output autospectrum for the concatenated pitch-rate time histories are shown in Fig. 6. The output spectrum follows the input spectrum at low input frequencies and exhibit the familiar 20 dB/decade roll-off at higher

frequencies (which is typical of rigid body motion). The cross-spectrum between elevator surface and pitch rate is shown in Fig. 7 and demonstrates a similar characteristic.

The elevator surface-to-pitch rate transfer function, q/δ_e, is shown in Figs. 8(a) and 8(b). The smooth spectral data over the majority of the frequency range are typical of the excellent results obtained from the Chirp z-transform algorithm. Due to the short period-mode excitation, there is a peak in the pitch-rate response at about 2.0 rad/sec, with an associated phase lag of 45 deg. At higher frequencies, the magnitude response rolls off at 20 dB/decade and the phase shift approaches -90 deg owing to the K/s pitch-rate characteristic and negligible flexibility/servo-lag effects. The drop in the magnitude response and associated positive phase response for frequencies below 0.3 rad/sec are due to the phugoid dynamics.

The coherence function shown in Fig. 9 is strong over the frequency range of interest (0.2-6.0 rad/sec), as shown. For input frequencies above 7.0 rad/sec, the coherence function becomes erratic and the transfer-function identification is less accurate. For low-frequency inputs (less than 0.3 rad/sec), the pitch-rate response decreases, even for the nearly constant input amplitude owing to the effect of the phugoid dynamics. This results in a decrease of information transfer and an associated drop in the coherence function. This coherence-function roll-off is also attributable to atmosphere turbulence effects, which become more important at low frequency where the turbulence spectrum peaks (Ref. [7]).

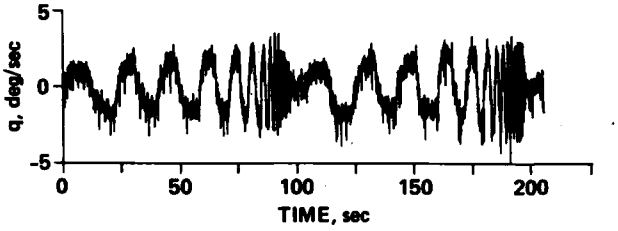

Figure 5. Pitch-rate response (q) during longitudinal frequency sweeps.

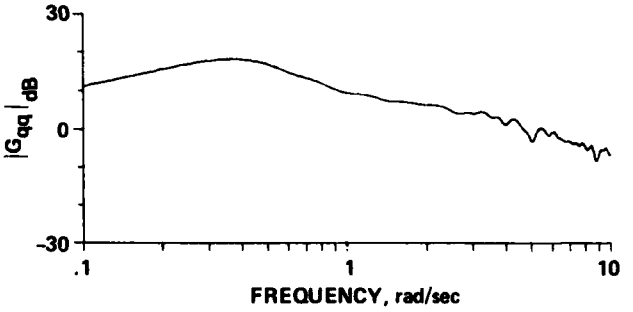

Figure 6. Pitch-rate output autospectrum (G_{qq}).

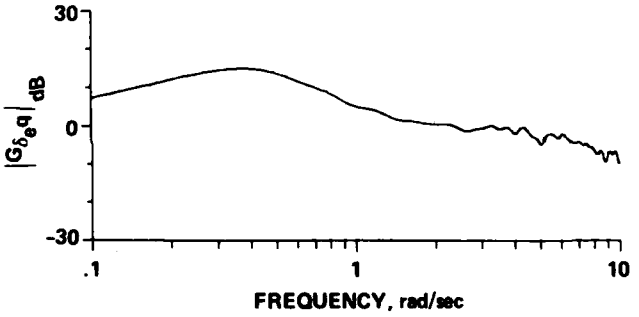

Figure 7. Magnitude of cross-spectrum between elevator surface inputs and pitch-rate response ($|G_{\delta_e q}|$).

The Bode plot of Figs. 8(a) and 8(b) is the basic format for presenting classical frequency-domain results. It provides useful information on dynamic characteristics and on handling qualities implications. To the extent that the linear-describing function is an accurate representation of the input-to-output process, the Bode plot is an exact description of the vehicle dynamics and contains no implicit assumptions on model order or structure. This is the key advantage of frequency-domain identification over the more conventional time-domain approaches.

Recent military specifications for piloted-handling qualities (Ref. [4]) are based on two key frequency-domain parameters: bandwidth (ω_{BW}) and effective time delay (τ_p). For a particular transfer function, the bandwidth is defined as that frequency where the phase margin is 45 deg, or the gain margin is 6 dB, whichever is lowest. As discussed in Ref. [4], the bandwidth is a measure of the speed of response; a high bandwidth reflects quick response and accurate tracking capability; a low bandwidth suggests sluggish response and pilot-induced oscillation tendencies. The effective time delay is a measure of the slope of the phase curve for frequencies near the bandwidth value. A large effective time delay (e.g., greater than 100 msec) results in a significant degradation of piloted handling qualities.

For longitudinal control, a key transfer function is pitch attitude response to elevator, θ/δ_e, which is easily derived from the pitch-rate transfer function as:

$$\frac{\theta(s)}{\delta_e(s)} = \frac{q(s)}{s\delta_e(s)} \tag{4}$$

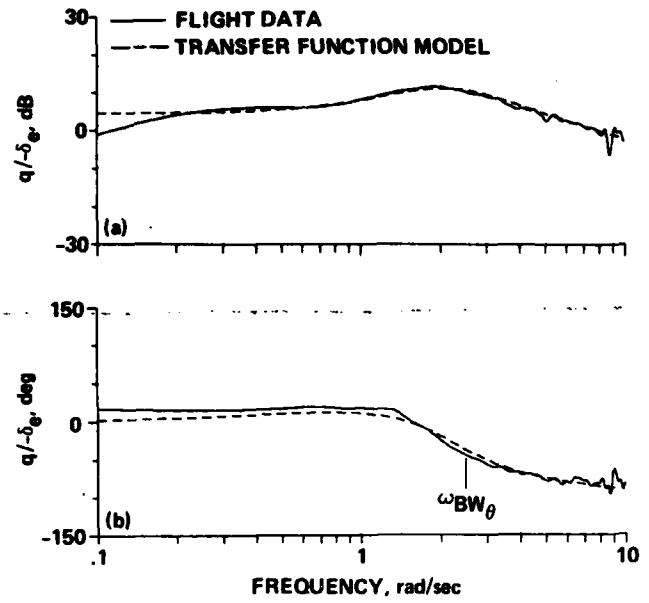

Figure 8. Pitch-rate response to elevator ($q/-\delta_e$) in cruise. (a) Transfer function magnitude. (b) Transfer function phase.

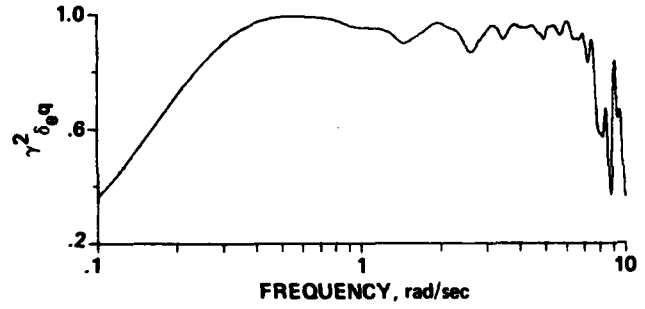

Figure 9. Coherence function for pitch-rate response identification ($\gamma^2_{\delta_e q}$).

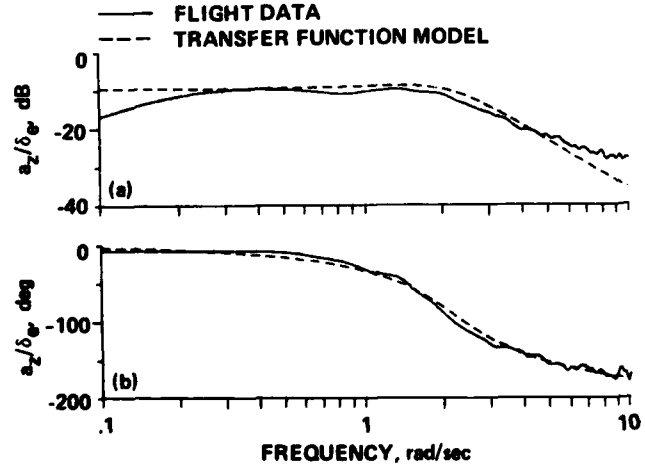

Figure 10. Vertical-acceleration response to elevator (a_z/δ_e) in cruise. (a) Transfer-function magnitude. (b) Transfer-function phase.

where s is the Laplace operator. The Bode plot for pitch-attitude response may be obtained from the pitch-rate response by rotating the magnitude curve about the $\omega = 1$ rad/sec point by slope of 20 dB/decade. The phase curve is shifted by a constant value of -90 deg. Referring to Fig. 8, the critical bandwidth criterion is phase margin which is 45 deg at a frequency of $\omega_{BW_\theta} = 2.5$ rad/sec. The effective time delay is negligible since the phase curve is nearly flat where it is near 180 deg. These bandwidth and time delay values are well within the Ref. [4] Level II, Category A, specifications (adequate handling qualities for high-precision tracking tasks), and certainly reflect satisfactory characteristics for SCAS failure conditions.

The transfer function for *normal acceleration response to elevator*, a_z/δ_e, is shown in Figs. 10(a) and 10(b). The response is dominated by the classical second-order short-period mode over the majority of the frequency range. The magnitude curve is flat at mid-frequency indicating a constant normal acceleration response to a step elevator input, with a roll-off in response for frequencies beyond the short period mode. The fall-off in normal acceleration response for frequencies below 0.3 rad/sec is probably due to the dominance of the phugoid dynamics. The phase curve exhibits the classical second order response; i.e., zero phase lag at low frequency, 180 deg of phase lag at high frequency, and 90 deg of phase lag at the second order mode ($\omega \doteq 2.0$ rad/sec). This is consistent with the previous pitch-rate results. The coherence function for the normal acceleration response shown in Fig. 11 is strong over the frequency range of 0.3 to 10.0 rad/sec, with the fall-off at low frequency, again owing to the dominance of phugoid dynamics and turbulence effects. As before, this suggests excellent identification over the entire frequency range of interest.

Longitudinal Transfer Function Fitting

Analytical transfer function forms are selected for each degree of freedom based on configuration and flight condition factors. In the hover flight condition, vehicle dynamics are dominated by the hovering cubic, and decoupled heave and yaw modes. In wing-borne flight, the conventional longitudinal and lateral quartic equations dominate. Thus, transfer-function models which are appropriate for the hover flight condition are not necessarily applicable to forward flight conditions. Obviously, if a model of high enough order is selected, the parameters can be adjusted to accommodate each flight condition. However, such transfer function models no longer

retain the physical significance of the classical lower-order parameters. Also, higher-order transfer-function models tend to be strongly tuned to the specific inputs which are used in the identification procedure (e.g., a frequency sweep) and are often very poor predictors of other test inputs (e.g., step inputs). Therefore, higher-order models are not desirable. In the approach taken in Ref. [3], the minimum-order transfer-function models which can satisfactorily fit the frequency responses are used with the upper limit taken as the physical order of the system.

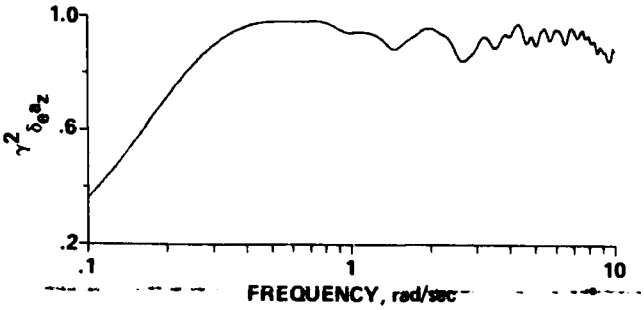

Figure 11. Coherence function for vertical-acceleration response identification ($\gamma^2_{\delta_e a_z}$).

Examination of the longitudinal frequency responses of Figs. 8(a) and 8(b) shows that the longitudinal dynamics of this flight condition are dominated by the short period mode (ω_{sp} = 2 rad/sec). Therefore, we adopt the classical pitch rate and normal acceleration responses to elevator*:

$$\frac{q(s)}{\delta_e(s)} = \frac{M_{\delta_e}(1/T_{\theta_2})e^{-\tau_\theta s}}{[\zeta_{sp},\ \omega_{sp}]} \tag{5}$$

where $q(s)/\delta_e(s)$ is the Laplace-transformed pitch rate response to elevator surface deflection, deg/sec/deg-elevator; M_{δ_e} is the elevator pitch sensitivity; $1/T_{\theta_2}$ is the first-order numerator inverse time constant; ζ_{sp}, ω_{sp} are the equivalent short-period mode damping and natural frequency, respectively; and τ_θ is the effective time delay; and

$$\frac{a_z(s)}{\delta_e(s)} = \frac{Z_{\delta_e} e^{-\tau_{a_z} s}}{[\zeta_{sp},\ \omega_{sp}]} \tag{6}$$

where $a_z(s)/\delta_e(s)$ is the Laplace-transformed vertical acceleration response (positive downward) to elevator surface deflection, g/deg-elevator; Z_{δ_e} is the elevator vertical sensitivity; and the denominator parameters are identical to those of Eq. (5). The effective time delay for the vertical acceleration response is τ_{a_z}.

We ignore the low-frequency phugoid dynamics since, as seen from Figs. 8 and 10, these are important only for the very lowest frequency inputs.

The longitudinal transfer functions of Eqs. (5) and (6) have the same denominator factors, so simultaneous fitting of these responses, while imposing the restriction of commonality of denominator parameters, makes good physical sense. Also, the analyses of Refs. [3] and [8], suggest that such simultaneous fitting techniques are needed to ensure unique and physically meaningful values for the numerator factors. For the longitudinal transfer functions, this avoids the otherwise so-called "fixed or free" L_α problem (Ref. [4]).

The transfer-function parameters of Eqs. (5) and (6) are iteratively varied in order to obtain a best least-squares fit between the equations and the frequency responses of Figs. 8 and 10 over the selected frequency range. This procedure is completed using the computer program LONFIT developed by Hodgkinson et al. (Ref. [9]). For the present case, the selected range for simultaneous fitting of the pitch rate and normal acceleration responses is 0.3 to 7 rad/sec. In this frequency range, the dynamics are clearly dominated by the short-period mode and the coherence is strong for both transfer functions. Once the short-period damping and natural frequency (ζ_{sp}, ω_{sp}) are obtained for the simultaneous fit, the high-frequency gain for the normal acceleration response (Z_{δ_e}) is varied holding the damping and frequency constant. This optimizes the a_z fit over the frequency range 0.3 to 10.0 rad/sec since the coherence function for this measurement remains strong out to higher frequencies. The transfer function parameters for the pitch rate and normal acceleration responses are finally obtained as:

*Shorthand notation: $[\zeta, \omega]$ implies $s^2 + 2\zeta\omega s + \omega^2$, ζ = damping ratio, ω = undamped natural frequency (rad/sec); and $(1/T)$ implies $s + (1/T)$, rad/sec.

$$
\left.
\begin{aligned}
M_{\delta_e} &= -7.727 \text{ deg/sec}^2\text{/deg-elevator} \\
&= -32.144 \text{ deg/sec}^2\text{/in.-}\delta_{LON} \\
1/T_{\theta_2} &= 1.035 \text{ rad/sec} \\
\zeta_{sp} &= 0.554 \\
\omega_{sp} &= 2.179 \text{ rad/sec} \\
\tau_\theta &= 0.016 \text{ sec}
\end{aligned}
\right\} \qquad (7)
$$

$$
\left.
\begin{aligned}
-Z_{\delta_e} &= 1.597 \text{ g/deg-elevator} \\
&= 6.644 \text{ g/in.-}\delta_{LON} \\
\zeta_{sp} &= 0.554 \\
\omega_{sp} &= 2.179 \text{ rad/sec} \\
\tau_{a_z} &= 0.018 \text{ sec}
\end{aligned}
\right\} \qquad (8)
$$

A comparison of these lower-order models with the flight test results is presented in Figs. 8 and 10. The pitch-response model matches the data very well over the selected fitting range (0.3-10.0 rad/sec for q/δ_e), which shows that the short period approximation adequately represents the high- and mid-frequency dynamics. For low-input frequencies ($\omega < 0.3$ rad/sec), the phugoid mode causes a drop in the pitch response, a characteristic which is not "captured" by the short period model. The match between the normal acceleration transfer function and the flight data is not nearly as good in the fitting range, and shows a noticeable discrepancy in the magnitude response for frequencies of greater than 2 rad/sec. Possible sources of the mid- and high-frequency discrepancy are the rotor rpm dynamics, which are known to be important for the forward flight conditions (Ref. [10]) and rotor inflow dynamics. Neither of these sources of added dynamics is directly accounted for by the classical short-period approximation, except to the extent that the short period parameters are adjusted in order to best fit the flight data. As in the pitch response, the low frequency mismatch is due to the omission of the phugoid mode from the transfer-function model.

Guidelines are given in the Mil Handbook (Ref. [4]) for the maximum allowable mismatch in lower-order system modeling. The discrepancies shown in the normal acceleration responses (Figs. 10(a) and 10(b)) are well within these allowable guidelines, so the identified parameters should be useful indicators of piloted-handling qualities. The capability to directly evaluate the effect of model order on response fitting is clearly seen in this example, again representing a unique advantage of the frequency domain approach. Further analyses could include the rotor rpm and phugoid degrees-of-freedom in the transfer-function models, and could evaluate their importance with respect to vehicle dynamics and handling qualities.

Lower order system parameters are useful in characterizing the vehicle dynamics for comparison with the dynamics of other aircraft. The identified short period damping and frequency ($\zeta_{sp} = 0.554$ and $\omega_{sp} = 2.18$ rad/sec) are consistent with preliminary observations which are based on the raw Bode plot information. The relatively high degree of damping is a reflection of the small response peak of the pitch-rate transfer function. The small effective time delays (in the pitch attitude and normal acceleration transfer fits) indicate that the high frequency flexibility and servo-lag effects are not important for this flight condition, as noted earlier. The Mil Handbook requirements for lower-order equivalent system pitch response are given in terms of the parameters $\omega_{sp}T_{\theta_2}$, ζ_{sp}, and τ_θ. The values of these parameters given in Eqs. (7) and (8) are well within the Level I, Category A, handling qualities requirements, confirming that the longitudinal characteristics for SCAS off conditions are adequate.

Time-domain verification of the longitudinal transfer function models will be addressed after lateral response models are presented.

Lateral Dynamics

The open-loop transfer function for *roll-rate response to ailerons* p/δ_a, is shown in Figs. 12(a) and 12(b). This is a classical first-order system in which aileron inputs produce a constant roll acceleration at high frequency, and a constant roll rate at low frequency. The corner frequency is about 1 rad/sec, with an associated phase lag of roughly -45 deg, as expected. The dominant time constant is thus roughly 1 sec, implying about 2 to 3 sec to reach a steady-state roll rate. The coherence function shown in Fig. 13 is very strong over the frequency range of 0.1 to 9.0 rad/sec, indicating an excellent identification of the roll-rate dynamics.

Specifications for the lateral handling qualities of military aircraft are given in the Mil Handbook (Ref. [4]), based on a lower-order equivalent-system model for the roll-attitude dynamics (ϕ/δ_a). When roll/yaw coupling is minor, the specification on the equivalent system roll mode time constant (T_r) can be interpreted as the reciprocal of the roll response bandwidth (ω_{BW_ϕ}). Referring again to Fig. 12(b), the bandwidth for *roll attitude* response to ailerons is ω_{BW_ϕ} = 0.9 rad/sec, yielding a dominant time constant of about 1.1 sec. This satisfies the Ref. [4] specification (T_r < 1.4 sec) for Level I, Category A, handling qualities.

Aerodynamic sideslip measurements are obtained from a sideslip indicator located roughly 18 ft ahead of the aircraft c.g. The sideslip at the c.g., β_{cg}, is calculated by correcting the measured signal for position error based on yaw rate and airspeed. No corrections are made for sensor dynamics because these are not felt to be significant within the identification bandwidth.

The transfer function for *sideslip response* (at the c.g.) *to rudder inputs* β_{cg}/δ_r, is shown in Figs. 14(a) and 14(b). The response is characterized by a lightly damped second-order mode with a frequency of about 1.6 rad/sec. High-frequency rudder inputs yield a constant sideslip acceleration, while low-frequency rudder inputs yield a constant sideslip angle corresponding to a steady-state yaw rate. The coherence function for this case, shown in Fig. 15 is strong over the frequency range 0.1 to 5.0 rad/sec, falling off sharply in the high frequency range.

The rapid and relatively low-frequency decline of the coherence function of Fig. 15 is unlike the previous transfer functions considered for the cruise flight condition. The reason for this difference is that aerodynamic sideslip is a state variable which is one derivative lower than the other rate variables considered previously. The response of parameters such as roll rate and pitch rate falls off at high frequency with a slope of 20 dB/decade. However, the aerodynamic sideslip response as seen in Fig. 14(a) falls off at the much faster rate of 40 dB/decade. Although the input autospectrum is roughly constant over the entire plotted frequency range, this rapidly falling response causes a marked reduction of the output autospectrum and cross-spectrum and an associated decline

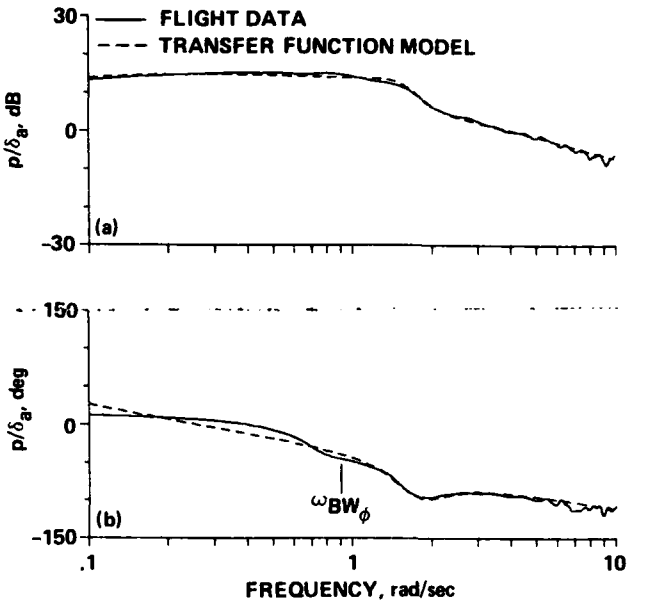

Figure 12. Roll-rate response to aileron (p/δ_a) in cruise. (a) Transfer-function magnitude. (b) Transfer-function phase.

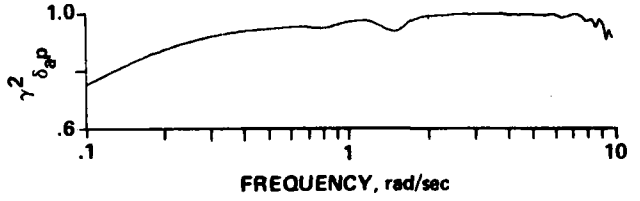

Figure 13. Coherence function for roll-rate response identification ($\gamma^2_{\delta_a p}$).

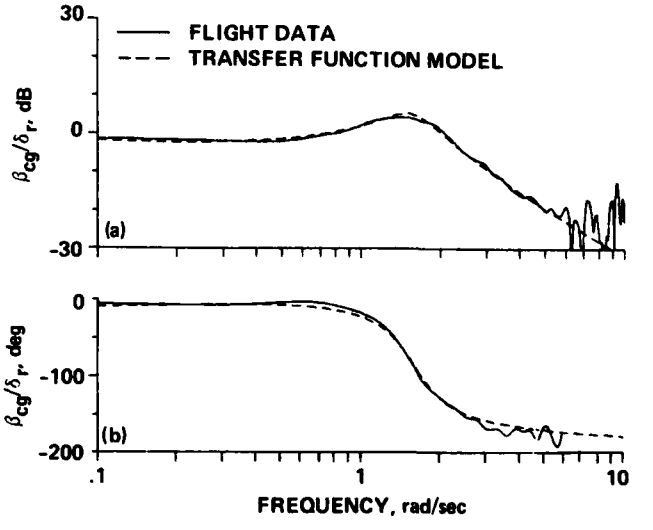

Figure 14. Sideslip response to rudder (β_{cg}/δ_r) in cruise. (a) Transfer-function magnitude. (b) Transfer-function phase.

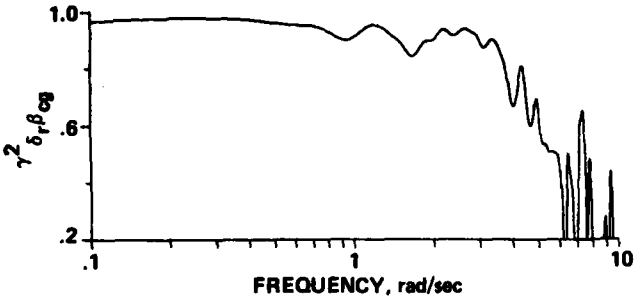

Figure 15. Coherence function for sideslip response identification ($\gamma^2_{\delta_r \beta_{cg}}$).

in the coherence function. This emphasizes the advantages of using the higher state derivatives in identifying the high-frequency dynamics and suggests the possible advantages of using attitude signals to identify the low-frequency dynamics. However, since the yaw mode of interest has a natural frequency of roughly 1.6 rad/sec, the falling coherence for frequencies greater than 5 rad/sec is not a severe limitation.

As in the roll axis, handling qualities specifications for the yaw axis response are given in terms of equivalent system models. These are derived in the following section.

Lateral Transfer Function Fitting

Equivalent system fitting using decoupled and coupled lateral/directional models has been considered in detail by Bischoff (Ref. [8]). With the *decoupled* model, the responses are fit independently, using a first-order roll rate and a second-order sideslip transfer function. The *coupled* model approach is based on simultaneous fitting of the roll and sideslip responses to obtain the following fourth-order transfer functions:

$$\frac{p(s)}{\delta_a(s)} = \frac{L_{\delta_a} s[\zeta_\phi, \omega_\phi] e^{-\tau_\phi s}}{(1/T_s)(1/T_r)[\zeta_d, \omega_d]} \tag{9}$$

where $p(s)/\delta_a(s)$ is the Laplace-transformed roll rate response to aileron surface deflection, deg/sec/deg-aileron; L_{δ_a} is the aileron roll sensitivity; ζ_ϕ, ω_ϕ are the second-order numerator damping and natural frequency, respectively; $1/T_s$, $1/T_r$ are the equivalent spiral and roll subsidence modes; ζ_d, ω_d are the equivalent Dutch roll mode damping and natural frequency, respectively; and τ_ϕ is the effective time delay.

$$\frac{\beta_{cg}(s)}{\delta_r(s)} = \frac{Y_{\delta_r}(1/T_{\beta_1})(1/T_{\beta_2})(1/T_{\beta_3}) e^{-\tau_\beta s}}{(1/T_s)(1/T_r)[\zeta_d, \omega_d]} \tag{10}$$

where $\beta_{cg}(s)/\delta_r(s)$ is the Laplace-transformed sideslip response to rudder surface deflection, deg/deg-elevator; Y_{δ_r} is the rudder sideslip sensitivity; $1/T_{\beta_1}$, $1/T_{\beta_2}$, $1/T_{\beta_3}$ are the first-order numerator inverse time-constants; and the denominator parameters are identical to those of Eq. (9). The effective time delay for the sideslip response is τ_β. The simultaneous fitting approach is consistent with that used in the longitudinal axis and allows the identification of the ω_ϕ/ω_d "coupling effect" in the roll response (Eq. (9), which is important in the handling qualities assessment.

The coherence function results of Figs. 13 and 15 show a satisfactory identification of both roll and sideslip responses in the frequency range of 0.1 to 5.0 rad/sec. Based on this fitting range, the computer program LATFIT (Ref. [11]) was used to obtain the parameters of Eqs. (9) and (10), simultaneously. Since the coherence for the *roll response* is satisfactory over the entire range of 0.1 to 10.0 rad/sec, this degree of freedom was refit alone, holding the denominator factors constant at the values obtained from the simultaneous solution. This procedure is analogous to that used in the longitudinal case and optimizes the values of the high-frequency gain and numerator parameters in the roll transfer function. The final results for the parameters of Eqs. (9) and (10) are:

$$\left.\begin{aligned} L_{\delta_a} &= 4.486 \text{ deg/sec}^2\text{/deg-aileron} \\ &= 17.630 \text{ deg/sec}^2\text{/in.-}\delta_{LAT} \\ \zeta_\phi &= 0.313 \\ \omega_\phi &= 1.887 \text{ rad/sec} \\ 1/T_s &= 0.063 \text{ rad/sec} \\ 1/T_r &= 1.090 \text{ rad/sec} \\ \zeta_d &= 0.248 \end{aligned}\right\} \tag{11}$$

$$\left.\begin{aligned} \omega_d &= 1.581 \text{ rad/sec} \\ \tau_\phi &= 0.045 \text{ sec} \end{aligned}\right\} \qquad (11)\ \text{(cont.)}$$

$$\left.\begin{aligned} Y_{\delta_r} &= -0.051 \text{ deg/sec/deg-rudder} \\ &= -0.408 \text{ deg/sec/in.-}\delta_{ped} \\ 1/T_{\beta_1} &= 0.086 \text{ rad/sec} \\ 1/T_{\beta_2} &= 0.818 \text{ rad/sec} \\ 1/T_{\beta_3} &= 47.946 \text{ rad/sec} \\ 1/T_s &= 0.063 \text{ rad/sec} \\ 1/T_r &= 1.090 \text{ rad/sec} \\ \zeta_d &= 0.248 \\ \omega_d &= 1.581 \text{ rad/sec} \\ \tau_\beta &= 0.026 \text{ sec} \end{aligned}\right\} \qquad (12)$$

The lateral/directional transfer function fits are plotted as dotted lines for comparison with the flight data of Figs. 12 and 14. The matching of the roll-response magnitude (Fig. 12) is excellent over the entire frequency range. Only a slight anomaly in the phase matching is apparent for low frequency inputs. The agreement between the sideslip fit and the flight data is also excellent (Fig. 14).

As a result of the simultaneous fitting of the roll and yaw responses, the transfer function parameters of Eqs. (9) and (10) have clearly retained their physical significance. The inverse roll mode time constant, $1/T_r = 1.090$ rad/sec is roughly equal to the roll response bandwidth as expected; both are well within the Level I roll response requirements, as mentioned earlier. The equivalent Dutch roll mode is lightly damped with a natural frequency roughly corresponding to the peak in the sideslip Bode magnitude plot (Fig. 14(a)). The small effective time delays for the roll and sideslip responses reflect negligible high-frequency flexibility and servo-lag effects, and are consistent with the previous longitudinal results. The small time delay in the sideslip response also supports the omission of corrections for sideslip sensor dynamics.

The ratio of the natural frequency of the numerator complex zero (ω_ϕ) to the denominator complex pole (ω_d) is one measure of roll/yaw coupling in response to aileron inputs. When $\omega_\phi = \omega_d$, the numerator and denominator quadratic factors roughly cancel, and the resulting decoupled roll response is characterized entirely by the roll-mode time constant. This case leads to the best handling qualities for a nominal value of the roll-mode time constant. As the roll/yaw coupling increases, the numerator and denominator quadratic factors of Eq. (9) no longer cancel and an undesirable oscillatory component of roll rate is generated. Referring to Eq. (11), the near unity value $\omega_\phi/\omega_d = 1.19$ suggests no such concern for roll/yaw coupling.

A more direct measure of the roll/yaw coupling is obtained from evaluating the ratio of roll attitude to sideslip evaluated at the Dutch roll frequency $|\phi/\beta|_d$. Analyses show (Ref. [4]) that there is a direct correlation between the $|\phi/\beta|_d$ ratio and the ratio of oscillatory roll rate to steady roll rate for step aileron inputs. A small value of $|\phi/\beta|_d$ (e.g., less than 1.4) suggests a small oscillatory roll-rate component and desirable handling qualities. A large value causes roll response overshoot and related poor tracking characteristics. A cross correlation of roll rate and sideslip responses yields $|\phi/\beta|_d = 1.27$, which implies no such tracking deficiencies. The preceding analyses have shown that the roll response is largely decoupled and first order in nature. Therefore, the simple, first-order roll rate model could be adopted for future studies.

4. Time Domain Verification of Transfer Function Models

The transfer function is the minimum realization description of a *linear* input-output process. The transfer-function models developed above can be used to generate all other frequency and time domain information. Therefore, a set of verified transfer function models is a useful output format for the linear identification procedure. However, the adequacy of these linearized transfer-function models for predicting the time-domain dynamics of *nonlinear* systems is at question. For such nonlinear systems, the transfer function is actually a describing function which is strictly valid only for the input amplitudes which were used in the flight test experiment. Also, since identification procedures tend to be tuned to the type of test inputs used (e.g., a sine-sweep), their accuracy in predicting responses to other classes of

inputs (e.g., steps, doublets) is often uncertain. Lastly, although the mismatches observed in the previous section between the transfer-function fits and the frequency-response flight data never exceeded the allowable handling quality specifications, the importance of these discrepancies in predicting time response behavior is still at issue. These questions are addressed in the following section.

The basic verification approach is to compare the step response of the aircraft with the response of the transfer-function model driven by the same recorded control inputs. The step responses were completed for all flight conditions with the stabilization system disengaged in order to show that the extracted transfer-function models are valid for the bare-airframe configuration. The transfer functions for the hover flight condition and those extracted in the present analysis for the cruise flight condition are summarized in Table 1. For illustrative consistency, all transfer functions are referenced to the three surface deflections: elevator, aileron, and rudder. The verification results for the hover flight condition are presented first.

TABLE 1.- SUMMARY OF IDENTIFIED TRANSFER-FUNCTION MODELS[a] FOR THE HOVER AND CRUISE FLIGHT CONDITIONS

Hover (V = 0)	Cruise (V = 170 knots, indicated)
Longitudinal dynamics	
$\frac{a_z}{\delta_c} = \frac{-0.108\ e^{-0.005s}}{(0.115)}$; g/in.– power lever	$\frac{a_z}{\delta_e} = \frac{1.597\ e^{-0.018s}}{[0.554,\ 2.179]}$; g/deg – elevator
$\frac{q}{\delta_e} = \frac{-2.607s(-0.075)(0.686)e^{-0.044s}}{(0.115)(1.597)[-0.978,\ 0.393]}$; deg/sec/deg – elevator	$\frac{q}{\delta_e} = \frac{-7.727(1.035)e^{-0.016s}}{[0.554,\ 2.179]}$; deg/sec/deg – elevator
Lateral dynamics	
$\frac{p}{\delta_a} = \frac{3.959s(-0.092)(0.570)e^{-0.022s}}{(0.108)(1.429)[-0.581,\ 0.427]}$; deg/sec/deg – aileron	$\frac{p}{\delta_a} = \frac{4.486s[0.313,\ 1.887]e^{-0.045s}}{(0.063)(1.090)[0.248,\ 1.581]}$; deg/sec/deg – aileron
$\frac{r}{\delta_r} = \frac{0.708\ e^{-0.019s}}{(0.108)}$; deg/sec/deg – rudder	$\frac{\beta_{cg}}{\delta_r} = \frac{-0.051(0.086)(0.818)(47.946)e^{-0.026s}}{(0.063)(1.090)[0.248,\ 1.581]}$; deg/deg – rudder
$\frac{r}{\delta_a} = \frac{0.398(-0.310)[0.762,\ 0.524]e^{-0.046s}}{(0.108)(1.429)[-0.581,\ 0.427]}$; deg/sec/deg – aileron	

[a]Shorthand notation: $[\zeta, \omega]$ implies $s^2 + 2\zeta\omega s + \omega^2$, ζ = damping ratio, ω = undamped natural frequency (rad/sec); and $(1/T)$ implies $s + (1/T)$, rad/sec.

Hover Flight Condition

A co-plot of the transfer-function model for yaw rate response to rudder r/δ_r (Table 1) *with the frequency response data of Ref. [3]* is presented in Fig. 16. The transfer-function model matches the flight data very well at high frequency in both magnitude and phase but not as well at low frequency. Even so, the fit meets the mismatch criteria of Ref. [4] for handling qualities assessment. These criteria emphasize the piloting crossover range of 1-3 rad/sec, in which the fit is excellent for this case.

When the transfer-function model is driven with one of the *swept sine-wave inputs* used in the identification procedure, the time-domain ramifications of model mismatch are clearly exposed. The transfer-function model and flight-data responses for a typical frequency sweep are compared in Fig. 17. The input amplitude shown in Fig. 17(a) is roughly ±20% of the maximum pedal travel producing a yaw response amplitude of roughly ±20 deg/sec, as seen in Fig. 17(b). The flat spot in the yaw rate signal at 50 sec is due to yaw-rate sensor limiting. In general, the match between the transfer-function response and the flight data is excellent. The phasing and form of the model response matches the flight data very well, with the only noticeable anomaly being an underestimation of the peak amplitudes for low-frequency inputs. This is a result of the fit mismatch at low frequency (Fig. 16). Thus, the transfer function model accurately captures the essence of the yaw-rate response over the frequency range of interest, and can be considered adequate for sine-wave type inputs.

The flight data for yaw rate response to a *step pedal input* is shown in Figs. 18(a) and 18(b). The control deflection represents roughly 40% of the maximum control power, a fairly large amplitude input. The maximum yaw-rate response is about 35 deg/sec, which is 75% greater than the peak values obtained in the frequency sweeps. The transfer-function model response co-plotted in the dashed curve of Fig. 18(b) compares extremely well with the flight data over the entire run—even for this fairly large input amplitude case. Analyses on the vertical response to collective (a_z/δ_c) showed the same excellent response correlation. This is expected since the response dynamics for the heave and yaw axes are nearly the same (Table 1).

The step-response run lengths of roughly 10 sec emphasize the high- and mid-frequency ranges, allowing only enough time for about one time constant (T_Y = 9.3 sec). Thus, the low-frequency mismatches never really have enough time to build up. This is typical of step-response data and illustrates the advantages of a symmetrical sine-sweep input. Clearly, however, the response in the first few seconds is the key concern of the pilot. This is reflected in the mismatch criteria being most stringent in the mid-frequency range.

So far, the time response results show that the simple transfer-function models match the step-response characteristics very well. Also, the use of a very low-order description has avoided any problems in over-tuned modeling. In general, however, good time history matching is highly dependent on the level of spurious inputs to the model due to: (1) improper setting of initial conditions, (2) control inputs required to suppress turbulence, and (3) unmodeled control coupling. When the model dynamics are *stable*, the effects of these spurious inputs die out with time, and response matching presents no particular problems. Such cases are the easiest for time-domain identification as well.

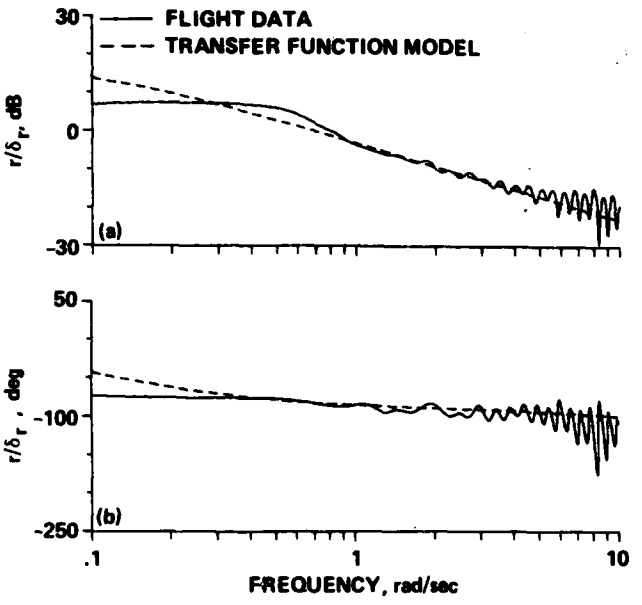

Figure 16. Yaw-rate response to rudder (r/δ_r) in hover. (a) Transfer-function magnitude. (b) Transfer-function phase.

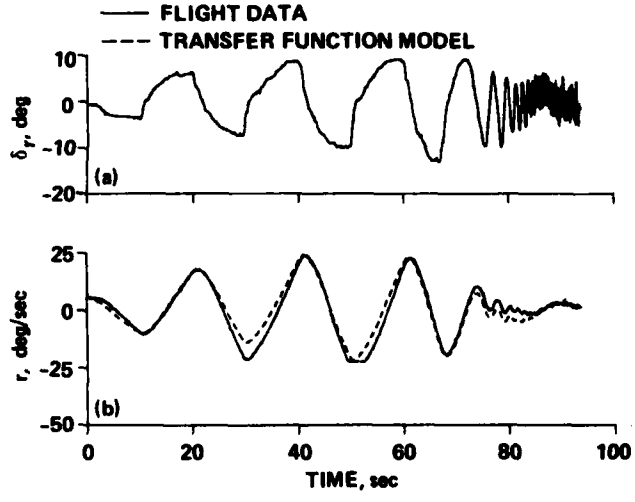

Figure 17. Comparison of aircraft and transfer-function model responses to a pedal frequency-sweep in hover. (a) Rudder surface deflection. (b) Yaw-rate response.

When the dynamics of the transfer-function response are *unstable*, the transients due to these spurious inputs grow with time. Therefore, small errors in the choice of initial conditions, or small inputs required to suppress the response to turbulence, can create gross differences between the transfer-function response and the flight data. Also, for unstable vehicles, acquisition and maintenance of a steady trim condition is often not possible, further complicating the proper initialization of the transfer function calculations. As the level of instability of the transfer-function dynamics increases, so do the problems of time-history matching. Not surprisingly, these are also the worst cases for time-domain identification.

The roll-rate-to-aileron transfer function (Table 1) is dominated by an unstable roll oscillation having a time-to-double of about 2.8 sec. This reflects the speed at which the errors and inexact control inputs and initial conditions will propagate. A good step response in the roll axis was achieved starting from a fairly steady initial trim condition as shown in Figs. 19(a) and 19(b). The assumed initial condition is determined from the average of the

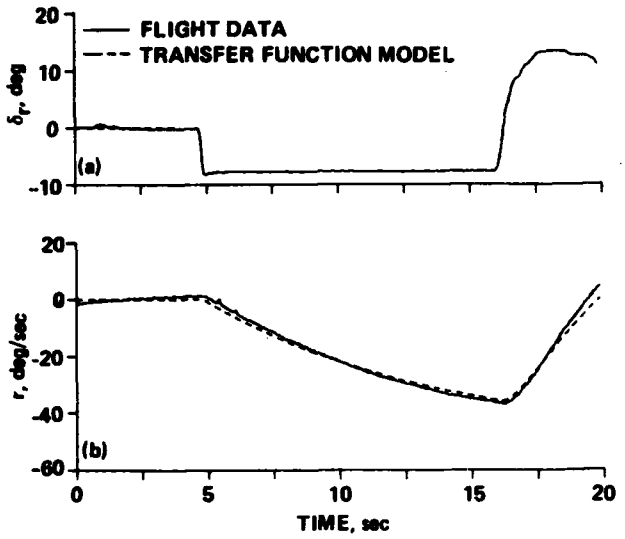

Figure 18. Comparison of aircraft and transfer-function model responses to a step rudder input in hover. (a) Rudder surface deflection. (b) Yaw-rate response.

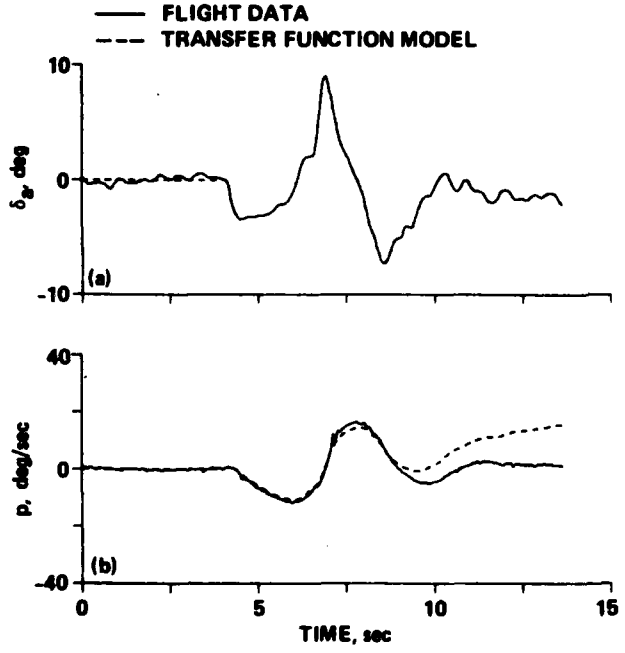

Figure 19. Comparison of aircraft and transfer-function model responses to a step aileron input in hover. (a) Aileron surface deflection. (b) Roll-rate response.

trim data as shown in the figures. The responses of the transfer function and flight data match very well for the first full cycle (4 sec) and begin to diverge after about 7 sec from the beginning of the step input. Even so, the form of the response as characterized by the relative damping, natural frequency, and amplitude is well modeled by the transfer function. The time histories diverge after about 7 sec, but this will not be important for such highly unstable systems (ζ_d = -0.581) since pilot regulation would obviously be applied within the first few seconds of the response; this again reflects the need to match properly mid- and high-frequency characteristics.

In the pitch axis, the effects of the unstable dynamics become far worse. The dominant pitch oscillation is very unstable (ζ_{sp} = -0.978, Table 1), having a time-to-double amplitude of 1.8 sec. This is almost half of the value for the roll axis. Acquisition and maintenance of a (mathematically) steady pitch trim in the hover flight condition is nearly impossible, even with the SCAS engaged. Also, the small pitch inputs needed to suppress turbulence responses cause a rapid divergence between the model and flight data time histories. Therefore, verification of the pitch response model is not feasible. This is a typical problem for identification schemes based on step inputs and further illustrates the advantages of using the symmetric swept sine-wave forms.

Cruise Flight Condition

As seen from the transfer-function models of Table 1, the dynamics of the cruise flight condition are very stable in comparison to those of the hover flight condition. None of the problems associated with initial condition matching or diverging transients was encountered in correlating the time histories for this flight condition. Unlike the hover flight condition, open-loop step responses were easily obtained and repeatable for all axes.

The pitch-rate response to step elevator deflection is shown in Figs. 20(a) and 20 (b). The elevator input corresponds to about 40% of the maximum control deflection. The comparison between the model response and the flight data is seen to be excellent over the majority of time history. The slight deviations occurring toward the end of the run are due to the inadequacy of the short period approximation in modeling the low-frequency (phugoid) dynamics (Fig. 8). Even so, the short period approximation clearly gives an excellent characterization of the important initial response dynamics.

The comparison of the transfer-function model and flight data for the normal acceleration response to the step elevator input of Fig. 20(a) is not nearly as good as it is in the pitch axis. This is mostly due to the mismatch between the assumed second-order model and the flight data at mid frequency (Fig. 10(a)). Referring to Fig. 20(c), the transfer function overpredicts the maximum acceleration response by nearly 40%. Despite this discrepancy, the initial response

slope, rise time, and percent overshoot are all well predicted; therefore, the transfer-function model is a useful characterization of the acceleration response. This comparison further indicates the need to investigate sources of unmodeled dynamics (e.g., engine response) in the vertical axis.

The aircraft roll rate response to a step aileron input is shown in Figs. 21(a) and 21(b). The transfer-function model shown in the dashed line accurately predicts that the response will be predominantly first order, with no overshoot or oscillatory tendency. This corroborates the same conclusion made earlier on the basis of the small ω_ϕ/ω_d and $|\phi/\beta|_d$ ratios. The sideslip response to a step rudder input is shown in Figs. 22(a) and 22(b) with the appropriate corrections for the nose-boom position. The transfer-function model shown in the dashed curve matches the flight data fairly well for the first 10 sec. Thereafter, the responses diverge, probably due to a gust encounter or some other aerodynamic interference effect at the sideslip vane during the recovery phase. Once again, the character of the step response is well predicted, with an accurate modeling of the rise time, overshoot, and steady state sideslip.

This verification study shows the utility of fairly simple transfer-function models in predicting the transient responses to relatively large and varied inputs. High-frequency and mid-frequency spectral response matching is clearly essential for accurate step response prediction, as it is for handling qualities assessments. Time response matching for unstable transfer functions is very difficult because of the inability to acquire and maintain a steady initial trim, and the tendency toward rapidly growing transients due to small unmodeled excitations.

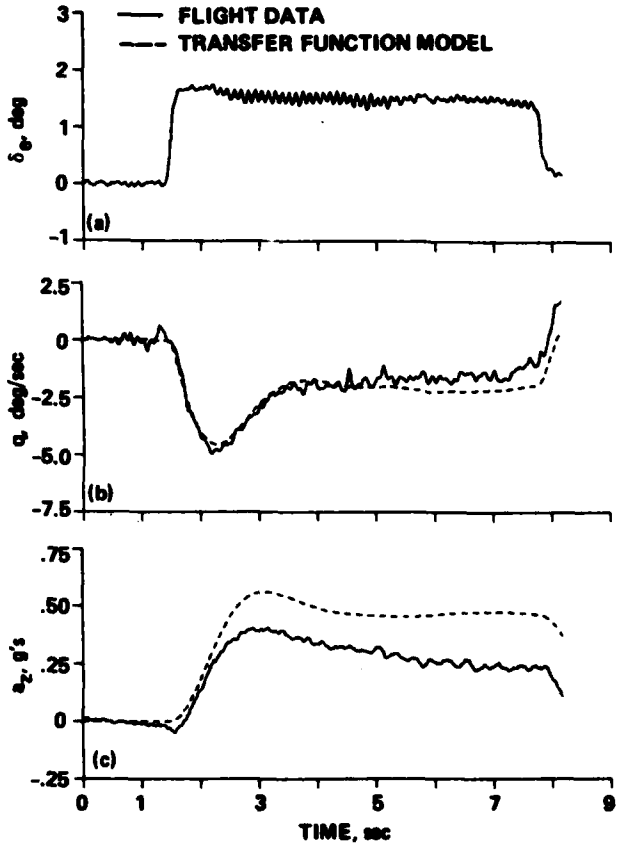

Figure 20. Comparison of aircraft and transfer-function model responses to a step elevator input in cruise. (a) Elevator surface deflection. (b) Pitch-rate response. (c) Normal (positive downward) acceleration response.

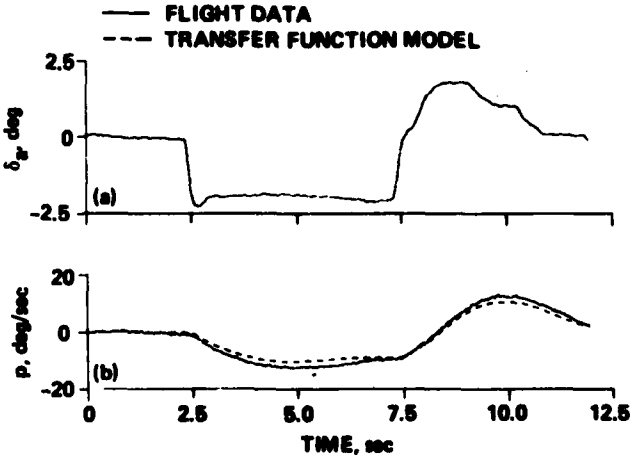

Figure 21. Comparison of aircraft and transfer-function model responses to a step aileron input in cruise. (a) Aileron surface deflection. (b) Roll-rate response.

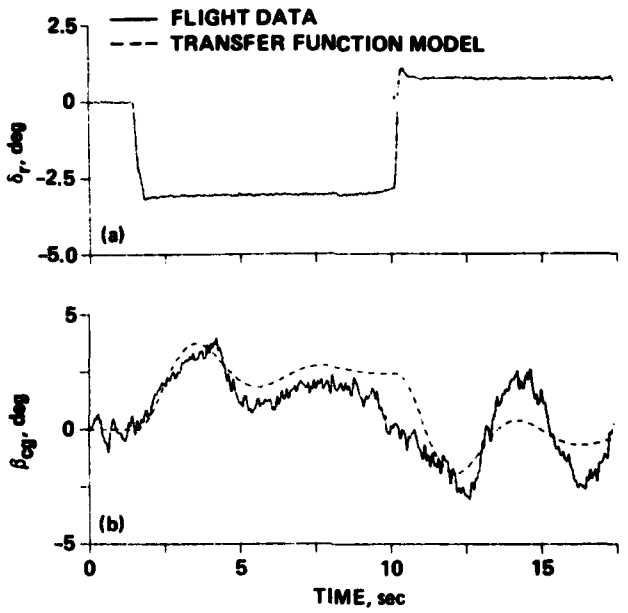

Figure 22. Comparison of aircraft and transfer-function model responses to a step rudder input in cruise. (a) Rudder surface deflection. (b) Sideslip response (at the c.g.).

5. Conclusions

Some specific conclusions from this study of the *open-loop* dynamics of the XV-15 tilt-rotor aircraft are:

1) The response characteristics for the cruise flight condition are very stable and decoupled. The handling quality parameters meet or exceed Level II, Category A, requirements for fixed-wing military aircraft.

2) Standard lower-order equivalent models adequately match the identified cruise dynamics in all degrees-of-freedom except for the normal acceleration responses to elevator deflection. The mismatch for this response is probably due to the unmodeled rotor rpm dynamics.

3) The step responses of the identified transfer functions and the aircraft generally match very well for both the hover and cruise flight conditions. Time-domain verification of the unstable attitude dynamics in hover is very difficult because small errors at the beginning of the run cause the responses of the model and the aircraft to diverge rapidly.

The frequency-domain approach has proven to be a relatively simple and accurate means for extracting the bare-airframe dynamics of the XV-15. The utility of the derived lower order transfer-function models for handling qualities and control-system studies has been shown in the frequency and time domains.

References

1) Samuel W. Ferguson, A Mathematical Model for Real-Time Flight Simulation of a Generic Tilt Rotor Aircraft, NAS2-11317, 1983.

2) N. N. Batra, R. L. Marr, and M. M. Joglekar, A Generic Simulation Model for Tilt Rotor Aircraft, Bell-Boeing Report 901-985-002, 1983.

3) Mark B. Tischler, Joseph G. M. Leung, and Daniel C. Dugan, Frequency-Domain Identification of XV-15 Tilt-Rotor Aircraft Dynamics, AIAA Paper 83-2695, Las Vegas, Nev., 1983.

4) Roger H. Hoh, David G. Mitchell, Irving L. Ashkenas, Richard H. Klein, Robert K. Heffley, and J. Hodgkinson, Proposed MIL Standard and Handbook—Flying Qualities of Air Vehicles, Vol. II: Proposed MIL Handbook, AFWAL-TR-82-3081, 1982.

5) Helicopter Flying and Ground Handling Qualities; General Requirements For, MIL-H-8501A, 1961.

6) Charles R. Chalk, David L. Key, John Kroll, Jr., Richard Wasserman, and Robert C. Radford, Background Information and User Guide for MIL-F-83300—Military Specification—Flying Qualities of Piloted V/STOL Aircraft, AFFDL-TR-70-88, 1971.

7) Bernard Etkin, The Turbulent Wind and Its Effect on Flight (AIAA Wright Brothers Lecture, 1980), UTIAS Review 44, Aug. 1980.

8) David E. Bischoff and Robert E. Palmer, Investigation of Low Order Lateral Directional Transfer Function Models for Augmented Aircraft, AIAA Paper 82-1610, San Diego, Calif., 1982.

9) M. E. Givan, W. J. LaManna, and J. Hodgkinson, LONFIT User's Guide, McDonnell Aircraft Company, Oct. 1978.

10) W. Earl Hall, Jr., J. G. Bohn, and R. S. Hansen, Preliminary Flight Test Planning for XV-15 Tilt Rotor Aircraft, Systems Control, Inc. Report CR-152392, Aug. 1979.

11) M. E. Givan, W. J. LaManna, and J. Hodgkinson, LATFIT User's Guide, McDonnell Aircraft Company, Oct. 1978.

A159470

1. Report No.	2. Government Accession No.	3. Recipient's Catalog No.
NASA TM 86009		

4. Title and Subtitle	5. Report Date
IDENTIFICATION AND VERIFICATION OF FREQUENCY-DOMAIN MODELS FOR XV-15 TILT-ROTOR AIRCRAFT DYNAMICS	August 1984
	6. Performing Organization Code

7. Author(s)	8. Performing Organization Report No.
Mark B. Tischler,* Joseph G. M. Leung and Daniel C. Dugan	A-9851
	10. Work Unit No. K-1585
9. Performing Organization Name and Address	11. Contract or Grant No.
*Aeromechanics Laboratory, U.S. Army Research and Technology Laboratories-AVSCOM, Ames Research Center and Ames Research Center, Moffett Field, CA 94035	13. Type of Report and Period Covered Technical Memorandum
12. Sponsoring Agency Name and Address	14. Sponsoring Agency Code
U.S. Army Aviation Systems Command, St. Louis, MO and National Aeronautics and Space Admn, Washington DC, 20546	

15. Supplementary Notes

Point of contact: Mark B. Tischler, Ames Research Center, MS 211-2, Moffett Field, CA 94035 (415) 965-5563 or FTS 448-5563

16. Abstract

Frequency-domain methods are used to extract the open-loop dynamics of the XV-15 tilt-rotor aircraft from flight test data for the cruise condition (V = 170 knots). The frequency responses are numerically fitted with transfer-function forms to identify equivalent model characteristics. The associated handling quality parameters meet or exceed Level II, Category A, requirements for fixed-wing military aircraft. Step response matching is used to verify the time-domain fidelity of the transfer-function models for the cruise and hover flight conditions. The transient responses of the model and aircraft are in close agreement in all cases, except for the normal acceleration response to elevator deflection in cruise. This discrepancy is probably due to the unmodeled rotor rpm dynamics. The utility of the frequency-domain approach for dynamics identification and analysis is clearly demonstrated.

Keywords:

17. Key Words (Suggested by Author(s))	18. Distribution Statement
XV-15 Tilt-Rotor aircraft; Parameter identification; Flight testing; Frequency-domain methods; Transfer function identification.	Unlimited Subject category: 08

19. Security Classif. (of this report)	20. Security Classif. (of this page)	21. No. of Pages	22. Price*
Uncl.	Uncl.	20	A02

*For sale by the National Technical Information Service, Springfield, Virginia 22161

END

FILMED

10-85

DTIC